Research Article

Molecular Docking and *in vivo* Toxicity Evaluations of Jopan Nanoherbal (*Clibadium surinamense* L.) Leaves in a Zebrafish Model

Dini Prastyo Wati
Postgraduate School, Study Program of Biology, Faculty of Mathematics and Natural Sciences, Universitas Sumatera Utara, Medan, Indonesia

Syafruddin Ilyas* and Elimasni
Study Program of Biology, Faculty of Mathematics and Natural Sciences, Universitas Sumatera Utara, Medan, Indonesia

Yurnadi Hanafi Midoen
Department of Medical Biology, Faculty of Medicine, Universitas Indonesia, Jakarta, Indonesia

* Corresponding author. E-mail: syafruddin6@usu.ac.id DOI: 10.14416/j.asep.2025.07.007
Received: 15 March 2025; Revised: 1 May 2025; Accepted: 5 June 2025; Published online: 15 July 2025

Abstract
Nanotechnological advancements have significantly increased the effectiveness of herbal remedies, particularly Jopan (*Clibadium surinamense* L.) leaves, which are recognised for their anti-inflammatory, antimicrobial, and antioxidant characteristics. This study aims to assess the toxicological potential of nanoherbal *C. surinamense* leaves via computational (molecular docking) and *in vivo* toxicity evaluations in a zebrafish model. ProTox-III was employed for the toxicity classifications; molecular docking simulations, using the CYP450 enzyme (PDB ID: 4R20); and *in vivo* zebrafish toxicity testing. Zebrafish were exposed to nanoherbal *C. surinamense* leaves at concentrations of 0, 12.5, 25, 50, 100, 200, 400, and 800 mg/L for 96 hours following OECD Guideline 203. The acute toxicity was evaluated by determining the LC50 value, while the toxic effects on the brain, liver, and intestinal tissues were assessed via histopathological analysis. An LC50 value of 516.87 mg/L was obtained, indicating low toxicity, while concentrations ≥200 mg/L caused dose-dependent toxic effects, including Purkinje cell degeneration, hepatocellular necrosis, and villus fragmentation. Molecular docking simulations revealed 2-undecanone 2,4-dinitrophenylhydrazone as the most active compound, exhibiting the strongest binding affinity (-7.4 kcal/mol) for CYP450. In conclusion, while nanoherbal *C. surinamense* leaves show therapeutic potential, their toxicity at higher concentrations necessitates further investigation to establish safe dosages; further, their long-term effects and pharmacokinetic properties should be explored to ensure their safety for medical applications.

Keywords: *C. surinamense*, *in vivo*, LC50, Molecular docking, Nanoherbal, Toxicity

1 Introduction

Nanotechnology has formed an important field of research for several decades and has diverse applications in areas such as electronics, medicine, materials science, and energy. Nanomaterials have been widely investigated with regard to various biomedical and biotechnological applications, including drug delivery, antibiotics, antibacterial agents, bioimaging, and tissue engineering, because of their unique physical and chemical features [1], [2], [3]. Nanotechnology in herbal pharmacology has led to the development of nanoherbal, enhancing the effectiveness and bioavailability of herbal medicines. For instance, nanoherbal from *Curcuma longa*, *Rhodomyrtus tomentosa*, *Bischofia javanica*, and

Phaleria macrocarpa utilise plant extracts known for their offering a variety of health benefits, such as anti-cancer, anti-inflammatory, and antioxidative effects [4]–[6]. The nanoscale dimensions and large surface area have led to concerns regarding their potential effects on biological health and the environment. This has prompted ongoing research to develop safe, sustainable options while investigating their applications across various fields.

The zebrafish (*Danio rerio*) is an important model organism in biomedical, pharmacological, and toxicological research due to its easy genetic modification and compatibility with fluorescent labelling, allowing for the real-time visualisation of biological structures and processes [7], [8]. Genetic alterations in zebrafish can produce fluorescent proteins that label specific cells or tissues, such as neurons and blood vessels, facilitating investigations of their development and functions. Zebrafish between the embryonic development and adult stages have emerged as a promising model in pharmacology and toxicology studies to quantify toxicity levels, perform targeted imaging, and evaluate disease progression through advanced bioimaging techniques, including confocal and two-photon microscopy [9], [10]. These capabilities allow high-precision drug screening, the development of novel treatments, and the evaluation of drug interactions on a cellular level. Furthermore, zebrafish are highly valued in various research fields, including developmental biology, genetics, drug discovery, and bioimaging, owing to their genetic adaptability, transparency, and physiological resemblance to humans [11].

Molecular docking is a computational modelling approach that provides insights into the interactions of compounds with a target receptor. It constitutes a key technique in toxicology, driving the characterisation of the binding processes and affinity of complex formation [12]. Molecular docking studies have shown that disinfection by-products (DBPs) can interact with vital proteins, including catalase (CAT), cytochrome P450 (CYP450), p53, and acetylcholinesterase (AChE), thus upsetting normal biological processes in zebrafish and corresponding to the toxic effects of DBPs [13]. CYP450 enzymes constitute a family of monooxygenases and are responsible for the oxidative metabolism of lipophilic drugs and xenobiotics. In this way, they mediate the metabolism of chemical compounds through both detoxification and bioactivation into reactive metabolites that can cause oxidative stress, DNA damage, and physiological disturbances, thus influencing toxicity [14], [15].

This research focuses on evaluating the toxicity of nanoherbal *C. surinamense* leaves towards zebrafish via acute toxicity bioassays to assess the safety of this plant-based treatment. Frequently used in traditional medicine, *C. surinamense* exhibits anti-inflammatory, antibacterial, and antioxidant properties, among other therapeutic effects. Since toxic agents – especially those derived from plant sources such as leaves, fruits, and other biological materials – can be passively transferred via direct contact, toxicology testing is vital in allopathic and alternative medicines to diagnose potential harmful effects before the appearance of symptoms from overconsumption. Zebrafish bioassays facilitate the assessment of dose-dependent responses, with zebrafish exhibiting genetic and neurological similarities to humans; furthermore, they are cost-effective, provide faster findings, and present greater ethical advantages compared to mammalian models [16]. Therefore, computational analysis and molecular docking, as well as toxicological evaluations, should be conducted to assess the safety of nanoherbal Jopan leaves, which is the main objective of this study. This study offers novel insights as it is the first to assess the toxicity of nanoherbal *C. surinamense* leaves through an integrated zebrafish bioassay and molecular docking approach, thereby contributing significant data for the advancement of safer nanoherbal medicines.

2 Materials and Methods

2.1 *Preparation of nanoherbal from jopan leaves (C. surinamense)*

C. surinamense leaves (101/K-ID/ANDA/I/2024) were collected from Padangsidimpuan, North Sumatra; dried and aired in a shaded area (without direct sunlight) for 1 week; and then ground into a coarse powder. Subsequently, the powder was processed further via planetary ball milling (PBM; PT. Nanotech Indonesia) in a 250-mL alumina container containing zirconium balls with diameters of 2 and 10 mm. The milling process was conducted for 20 h at 500 revolutions per minute (rpm) to achieve a uniform particle size distribution.

2.2 *In silico simulations*

2.2.1 Bioactive substances in nanoherbal C. surinamense leaves

In a previous study, 9 compounds were obtained from the methanolic nanoherbal leaf extract of *C. surinamense* [17]. These compounds were selected based on their molecular weight (≤500 g/mol) and their three-dimensional structures retrieved from the PubChem database (https://pubchem.ncbi.nlm.nih.gov/); all passed the Lipinski criteria with zero violations. The identified compounds include methanamine (PubChem CID: 6329), 8-(2-acetyloxiran-2-yl)-6,6-dimethylocta-3,4-dien-2-one (PubChem CID: 539293), 4-hydroxy-3-methyl-2-(2-propenyl)-2-cyclopenten-1-one (PubChem CID: 11083), 2-undecanone 2,4-dinitrophenylhydrazone (PubChem CID: 5717665), 1,5,5-trimethyl-6-[2-(2-methyl-[1,3]dioxolan-2-yl)-vinyl]-4-methylene-7-oxa-bicyclo[4.1.0]hept-2-ene (PubChem CID: 5368073), 6-tridecene (PubChem CID: 138758), hexadecanoic acid, methyl ester (PubChem CID: 8181), 2-cyclopentene-1-undecanoic acid (PubChem CID: 110680), and cyclopentaneundecanoic acid, methyl ester (PubChem CID: 535041).

2.2.2 Toxicity evaluation

The toxicities of the 9 compounds, including the nanoherbal leaf formulation of *C. surinamense*, were assessed using the ProTox 3 web server (https://tox-new.charite.de/protox_III/). Additionally, their potential to induce hepatotoxicity, carcinogenicity, immunotoxicity, mutagenicity, and cytotoxicity was analysed using ProTox 3.0 [18].

2.2.3 Protein preparation and molecular docking

The structure of CYP450 (PDB ID: 4R20), obtained from the RCSB Protein Data Bank (https://www.rcsb.org/) and depicted in Figure 1, illustrates Chain A of CYP450, which contains the active site. This protein is complexed with abiraterone as its native ligand, serving as the control in this study. The protein was prepared by removing water molecules and native ligands using Discovery Studio 2019. Subsequently, the selected bioactive compounds from nanoherbal *C. surinamense* leaves were optimized and energy-minimized using Open Babel in PyRx 0.8, and converted to pdbqt format as ligands. The molecular docking process was conducted using AutoDock Tools integrated in PyRx 0.8, employing a diverse ligand library [19].

The active site of the protein targeted in the docking involved the residues ASN209, GLU298, THR310, THR361, and MET396 [20]. The grid box was configured to encompass the active residues, with dimensions of 35.84 × 25.00 × 78.59 Å and centered at coordinates (x = 5.91), (y = 6.78), and (z = 25.44). Upon completion of the docking process, PyMOL was utilized to visualize the interaction between the ligand and protein, ensuring that the ligand's position in the active site corresponded with the docking results. The docking results were analyzed based on the binding affinity, which indicates the strength of the interaction between the ligand and protein. The binding affinity value reflects the effectiveness of the bioactive compound in binding to the active site of the protein, with lower values indicating higher affinity. Further interactions between the bioactive compounds and the proteins were visualized using Discovery Studio 2019 [21], [22].

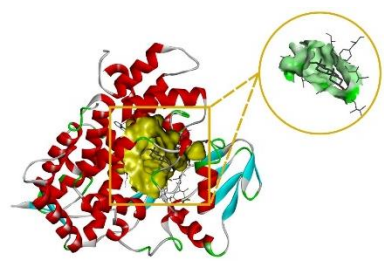

Figure 1: Active site visualization of CYP450 protein (Chain A, 4R20).

2.3 *Animal experimentation*

The zebrafish utilized in this study were healthy adult specimens (approximately 3 months old, with an average length of 2.5–3 cm) obtained from a local supplier in Medan, Indonesia. Upon arrival, they were quarantined in a recirculating aquaculture system within a 20 L aquarium to acclimate them to laboratory conditions. The system was maintained at a constant temperature of 26 °C and followed a 14:10-hour light–dark cycle. Water that was dechlorinated and purified through reverse osmosis was used. During the quarantine and experimental phases, the zebrafish were fed brine *Shrimp nauplii* twice daily to maintain their health and well-being of the fish. The experimental setup included eight aquariums, one serving as the control and the remaining used for testing; each

contained 4 L of reconstituted water and housed seven adult zebrafish to maintain consistent density. The zebrafish used in this study were not separated by sex, as the sex ratio has been reported not to significantly influence the outcomes of acute toxicity assessments. All procedures involving zebrafish followed the ethical guidelines sanctioned by the Animal House, FMIPA, Universitas Sumatera Utara, with an ethical approval number of 0030/KEPH-FMIPA/2025.

2.4 *Evaluation of acute toxicity*

The toxicity of the nanoherbal Jopan leaves was evaluated using a zebrafish model according to OECD Guideline 203 [23]. The fish were exposed to various test substance concentrations (0, 12.5, 25, 50, 100, 200, 400, and 800 mg/L) for 96 h, with mortality observations made at 24, 48, 72, and 96 h [10], [24]. This study applied the static exposure method, where each concentration was tested using 10 healthy fish replicates in each experimental group. The mortality was assessed based on the absence of movement and response to touch on the caudal peduncle. The LC50 value – the concentration leading to 50% mortality – was determined by recording the number of fish that died at each concentration during the test exposure period with a 95% confidence limit, calculated through probit regression analysis using the Statistical Package for Social Sciences (SPSS) Statistics 30.0.0 software [25].

2.5 *Histopathological profiling in zebrafish model to assess acute toxicity*

In the histopathological evaluation of nanoherbal *C. surinamense* leaves for studying acute toxicity using zebrafish, tissue samples were taken from significant organs, including the brain, liver, and intestine, after a 96-hour exposure period. The tissues were fixed using 10% formalin and then dehydrated and embedded in paraffin for sectioning. The resulting thin sections were treated with hematoxylin and eosin (H&E) stain and examined under a light microscope (Olympus CX43) to evaluate cellular and structural changes. This analysis focused on identifying common signs of toxicity, including cell degeneration, necrosis, inflammation, and structural disruption, within the brain, liver, and intestines to determine the impact of nanoherbal *C. surinamense* leaves exposure at various concentrations. Histological observations were conducted to examine the physiological effects of nanoherbal Jopan, which contributed to the overall toxicity assessment.

3 Results and Discussion

3.1 *Molecular docking simulations*

3.1.1 Toxicity predictions

The toxicities of nine potentially active compounds from nanoherbal *C. surinamense* leaves were evaluated using toxicity prediction data. According to toxicity classifications, the compound methanamine falls in toxicity class 3, with a lethal dose 50 (LD50) of 100 mg/kg, indicating high toxicity. In contrast, 8-(2-acetyloxiran-2-yl)-6,6-dimethylocta-3,4-dien-2-one belongs to toxicity class 4, with an LD50 of 1190 mg/kg. Other compounds – such as 4-hydroxy-3-methyl-2-(2-propenyl)-2-cyclopenten-1-one, 2-undecanone 2,4-dinitrophenylhydrazone, and cyclopentaneundecanoic acid, methyl ester – are in toxicity class 5, with LD50 values of 2900, 3000, and 5000 mg/kg, respectively, indicating lower toxicity levels (Figure 2(a)). These compounds are classified into toxicity categories ranging from harmful to non-toxic, emphasising their diverse pharmacological properties and the importance of distinguishing them for therapeutic use [26]. This classification is based on the Globally Harmonised System of Classification and Labelling of Chemicals (GHS), categorising compounds into classes I to VI according to their LD50 values in mice [27], [28].

Most bioactive compounds from *C. surinamense* fall into toxicity classes 4 and 5, indicating that they may be harmful or possibly harmful if ingested, though they are relatively safer compared to compounds in lower toxicity classes. This prediction provides valuable insights for further *in vivo* studies with regard to determining safe experimental doses. Notably, 2-cyclopentene-1-undecanoic acid, with an LD50 of 48 mg/kg, falls in toxicity class 2, indicating significantly high toxicity. Furthermore, many of these compounds show the potential for organ toxicity, such as hepatotoxicity, respiratory toxicity, carcinogenicity, mutagenicity, blood–brain barrier (BBB) penetration, and ecotoxicity (Figure 2(b)).

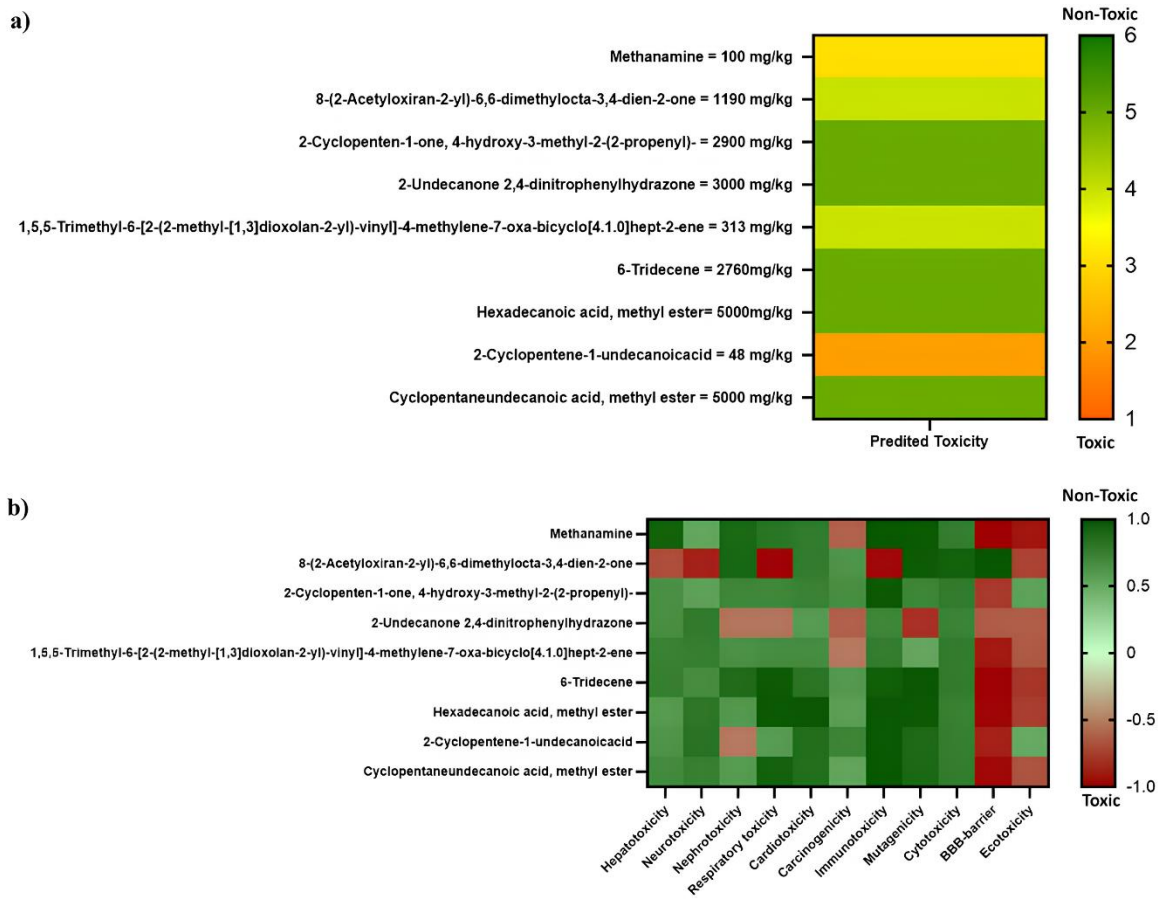

Figure 2: Toxicity and prediction of nine potential compounds. (a) Classification of toxicity based on toxicity classes and estimated LD50 values. (b) The probability of inducing various types of toxicity.

3.1.2 Molecular docking

This study applied molecular docking to evaluate the molecular interactions between compounds from nanoherbal *C. surinamense* leaves and CYP450 proteins. This technique allows one to model ligand interactions with biological receptors and analyse the stability of binding complexes, providing mechanistic insights into compound toxicity. The stability of ligand–receptor connections was measured using the binding energy, which indicates the existence of hydrogen bonding, electrostatic, and hydrophobic interactions [29], [30]. Previous studies have demonstrated that CYP450 enzymes increase zebrafish toxicity by converting *N*-nitrosodiethylamine into reactive metabolites, which cause oxidative stress and cellular damage [31]. Two of the nine tested compounds of nanoherbal *C. surinamense* leaves demonstrated a high affinity for the target CYP450 protein, indicating a possible role in modifying CYP450 enzymatic activity.

The binding affinities and residue interactions are detailed in Table 1. The binding affinity of all compounds derived from the nanoherbal leaves of *C. surinamense* was observed to be lower than that of the control ligand, abiraterone (-9.2 ± 0.40 kcal/mol). However, the binding affinities of the nanoherbal compounds were ranked as follows: 2-Undecanone 2,4-dinitrophenylhydrazone (-7.4 ± 0.12 kcal/mol) > 1,5,5-Trimethyl-6-[2-(2-methyl-[1,3]dioxolan-2-yl)-vinyl]-4-methylene-7-oxa-bicyclo[4.1.0]hept-2-ene (-6.8 ± 0.14 kcal/mol) > 8-(2-Acetyloxiran-2-yl)-6,6-dimethylocta-3,4-dien-2-one (-5.6 ± 0.13 kcal/mol) > 2-Cyclopentene-1-undecanoic acid (-5.5 ± 0.10 kcal/mol) > Cyclopentaneundecanoic acid, methyl ester (-5.4 ± 0.50 kcal/mol) > 6-Tridecene (CAS) (-5.2 ± 0.35 kcal/mol) > 2-Cyclopenten-1-one, 4-hydroxy-3-methyl-2-(2-propenyl)-(-5.1 ± 0.20 kcal/mol) >

Hexadecanoic acid, methyl ester (-4.6 ± 0.07 kcal/mol) > Methanamine (-1.6 ± 0.10 kcal/mol). The closer the binding affinity of the bioactive compounds approaches that of the native control ligand Abiraterone to the CYP450 protein, the greater the potential for toxicity [32]. Based on these findings, 2-Undecanone 2,4-dinitrophenylhydrazone exhibited the highest binding affinity after the control, with a value of -7.4 ± 0.12 kcal/mol, indicating a stronger potential interaction with the CYP450 protein and a likely higher toxicity effect. Furthermore, 1,5,5-Trimethyl-6-[2-(2-methyl-[1,3]dioxolan-2-yl)-vinyl]-4-methylene-7-oxa-bicyclo[4.1.0]hept-2-ene (-6.8 ± 0.14 kcal/mol) and 8-(2-Acetyloxiran-2-yl)-6,6-dimethylocta-3,4-dien-2-one (-5.6 ± 0.13 kcal/mol) also demonstrated relatively high binding affinities, suggesting significant potential interactions with CYP450. Although their binding affinities were slightly lower than that of 2-Undecanone 2,4-dinitrophenylhydrazone, these compounds still exhibited the possibility of toxic effects, albeit not as pronounced as those with higher binding affinities.

Table 1: Residues and binding energies of *C. surinamense* leaf nanoherbs interacting with CYP450.

No	Compound	PubCem ID	Interaction with				Binding Affinity (kcal/mol)
			Conventional hydrogen bond	Carbon hydrogen	Van der Waals	Hydrophobic	
1	Abiraterone (Control Ligand)	132971	SER367	ASN209	-	LEU112, ALA120, PHE121, ILE212, ALA302, ILE371, VAL480	-9.2 ± 0.40
2	Methanamine	6329	THR309, GLU305	-	-	-	-1.6 ± 0.10
3	8-(2-Acetyloxiran-2-yl)-6,6-dimethylocta-3,4-dien-2-one	539293	ARG103, SER367	CYS440	-	LEU370, ILE371, HIS373	-5.6 ± 0.13
4	2-Cyclopenten-1-one, 4 -hydroxy-3-methyl-2-(2-propenyl)-	11083	-	-	-	CYS440, ALA446, LEU450	-5.1 ± 0.20
5	2-Undecanone 2,4 -dinitrophenylhydrazone	5717665	AGR246, ALA297	GLY301	ALA297	LEU112, ALA302	-7.4 ± 0.12
6	1,5,5-Trimethyl-6-[2-(2-methyl-[1,3]dioxolan-2-yl)-vinyl]-4-methylene-7-oxa-bicyclo[4.1.0]hept-2-ene	5368073	ALA302	ASN209, GLU305	-	ALA120, ALA302, VAL213, VAL480, VAL481	-6.8 ± 0.14
7	6-Tridecene(CAS)	138758	-	-	-	ILE212	-5.2 ± 0.35
8	Hexadecanoic acid, methyl ester	8181	-	MET294	-	VAL213, ALA297, VAL480	-4.6 ± 0.07
9	2-Cyclopentene-1-undecanoicacid	110680	ARG246	-	-	VAL213, VAL480	-5.5 ± 0.10
10	Cyclopentaneundecanoic acid, methyl ester	535041	-	GLY301	-	LEU112, ILE212	-5.4 ± 0.5

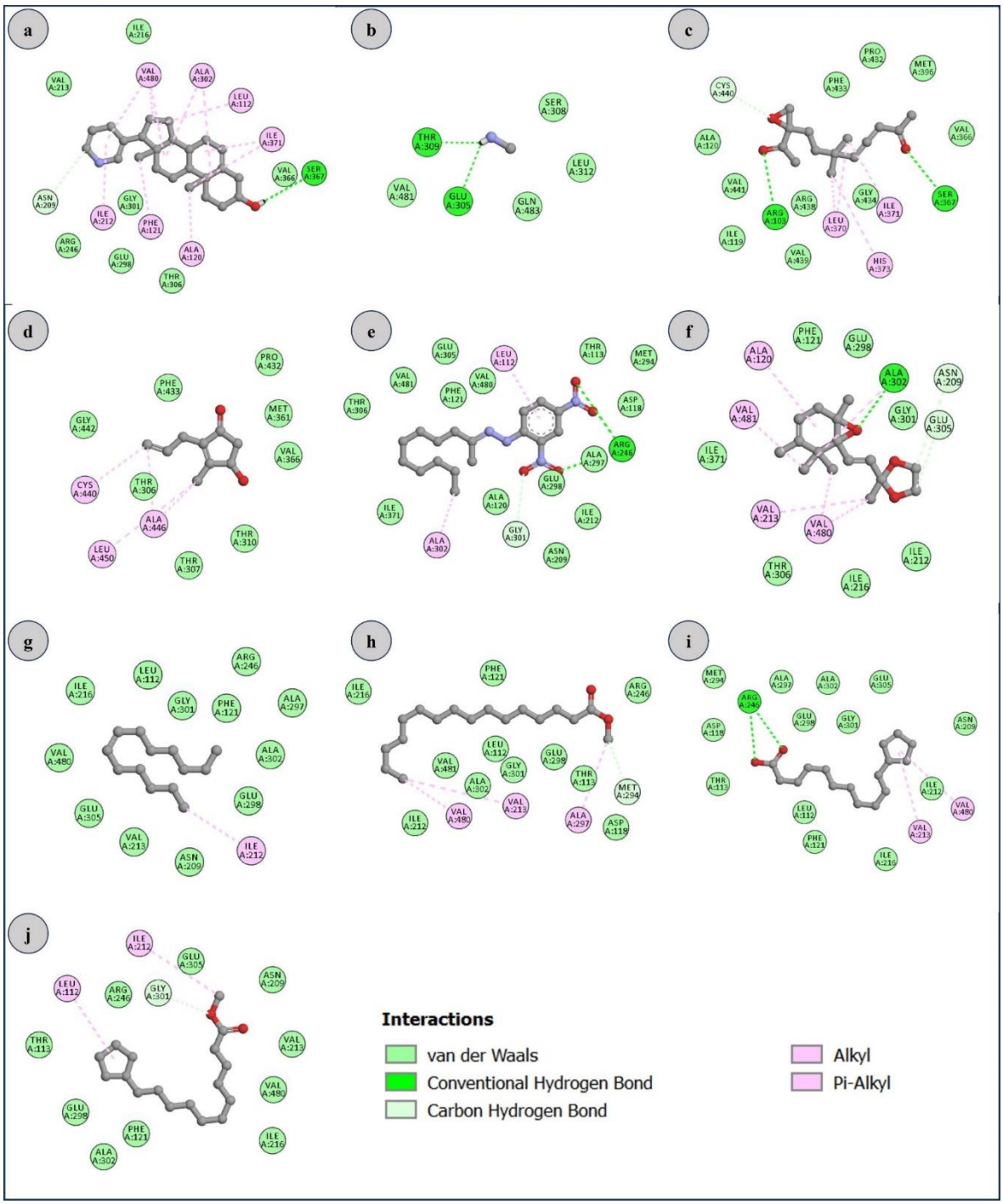

Figure 3: 2D Visualizations of Interactions Between CYP450 and nanoherbal *C. surinamense* Leaves compounds: (a) abiraterone (b) Methanamine (c) 8-(2-Acetyloxiran-2-yl)-6,6-dimethylocta-3,4-dien-2-one (d) 2-Cyclopenten-1-one,4-hydroxy-3-methyl-2-(2-propenyl)- (e) 2-Undecanone2,4-dinitrophenylhydrazone (f) 1,5,5-Trimethyl-6-[2-(2-methyl-[1,3]dioxolan-2-yl)-vinyl]-4-methylene-7-oxa- bicyclo[4.1.0]hept-2-ene (g) 6-Tridecene (CAS) (h) Hexadecanoic acid, methyl ester (i) 2-Cyclopentene-1-undecanoic acid (j) Cyclopentaneundecanoic acid, methyl ester.

The molecular docking analysis of the CYP450 protein with bioactive compounds derived from nanoherbal *C. surinamense* leaves revealed the establishment of diverse interactions, including conventional hydrogen bonds, carbon-hydrogen bonds, Van der Waals forces, and hydrophobic interactions, such as alkyl and Pi-alkyl, as illustrated in Figure 3 and Table 1. Conventional hydrogen bonding significantly enhances the binding affinity between the ligand and the protein, while carbon-hydrogen bonding and Van der Waals forces contribute to the stabilization of the complex by fortifying interactions between polar and non-polar molecules. Hydrophobic interactions, including alkyl and Pi-alkyl, are crucial in reinforcing the interaction with the protein through hydrophobic contacts, thereby increasing the stability of the ligand-protein complex in aqueous environments. In the control (abiraterone), conventional hydrogen bonds were observed at the SER367 and ASN209 residues, along with hydrophobic interactions at the LEU112, ALA120, PHE121, ILE212, ALA302, ILE371, and VAL480 residues. Among the bioactive compounds evaluated, 2-Undecanone 2,4-dinitrophenylhydrazone and 1,5,5-Trimethyl-6-[2-(2-methyl-[1,3]dioxolan-2-yl)-vinyl]-4-methylene-7-oxa-bicyclo[4.1.0]hept-2-ene exhibited the highest binding affinities, with values of -7.4 ± 0.12 kcal/mol and -6.8 ± 0.14 kcal/mol, respectively, which are comparable to the control binding affinity. Both compounds formed hydrogen bonds with key residues, such as ALA297, GLY301, and ASN209, and engaged in hydrophobic interactions with residues, such as ALA120, ALA302, VAL213, and VAL480. The interaction patterns akin to those of the control ligand suggest a binding mechanism analogous to that of the CYP450 protein. These interactions enhance the stability of the ligand-protein complex, potentially augmenting the bioactivity of the compounds. The results demonstrate robust hydrogen bonding and hydrophobic interactions, indicating the high potential of these compounds to modulate the enzymatic activity of the CYP450 protein, which is pivotal for the metabolism of xenobiotic species in organisms [33]. In molecular docking modeling, a higher binding affinity corresponds to a lower binding energy [34]. Consequently, the low binding energies of these compounds imply a stronger affinity for CYP450, indicating a substantially higher potential effect on the enzymatic activity of this protein. However, the formation of strong bonds at the active site of the CYP450 enzyme could also impact the function of enzymatic metabolism, potentially leading to toxicity. Therefore, while both bioactive compounds from nanoherbal *C. surinamense* exhibit good affinity, their toxicity potential should be further evaluated to assess their possible impacts on biological systems.

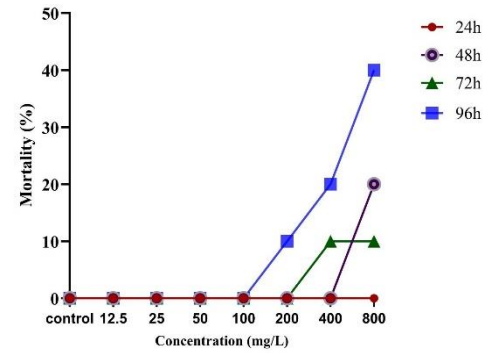

(a)

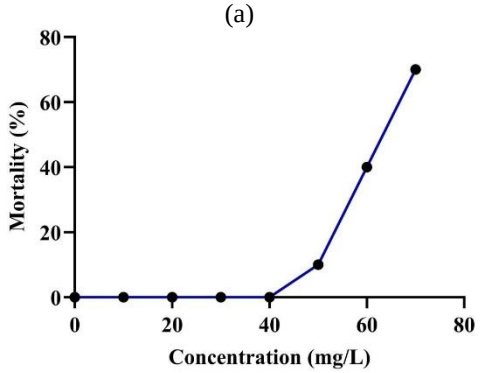

(b)

Figure 4: Mortality of zebrafish: (a) Hourly observation of zebrafish mortality rate at 24, 48, 72, and 96 h following exposure to nanoherbal *C. surinamense* leaf (b) Cumulative LC_{50} values of nanoherbal *C. surinamense* leaf over time.

3.2 *Acute toxicity*

In assessing the toxicity of nanoherbal *C. surinamense* leaves towards adult zebrafish at concentrations of 0 (control), 12.5, 25, 50, 100, 200, 400, and 800 mg/L over time intervals of 24, 48, 72, and 96 hours, the mortality rates were determined by the deceased fish count in each treatment group (Table 2). Low concentrations (12.5–100 mg/L) prove relatively safe for zebrafish, with no mortality recorded up to 96 hours of exposure. However, at a moderate concentration (200 mg/L), the mortality rate is 10% after 96 h, indicating mild toxicity. At a concentration of 400 mg/L, the mortality rises significantly to 40%

after 96 h of exposure. Mortality is manifested at 72 h, indicating that the toxic effects accumulate progressively. At a concentration of 800 mg/L, the mortality reaches 70% after 96 hours, with a gradual increase from 10% at 48 h to 40% at 72 h. Figure 4(a) depicts a direct correlation, where escalating doses affect the mortality rate in zebrafish. The results align with existing literature, indicating that elevated concentrations of herbal substances frequently correspond with increased toxicity [35], [36], [37].

The LC50 value of the nanoherbal *C. surinamense* leaves in zebrafish reveals a significant increase in toxicity over time. At 24 h, no mortality was observed; thus, the LC50 value could not be determined because the fish remained unaffected at concentrations below 200 mg/L (Table 2). Exposure to 400 mg/L resulted in a significant increase in mortality, reaching 40% after 96 h. Mortality is manifested at 72 h, indicating that the toxic effects accumulate progressively. At a concentration of 800 mg/L, the mortality reaches 70% after 96 h, with a progressive increase from 10% at 48 h to 40% at 72 h. Figure 4(b) depicts a direct correlation, where escalating doses affect the mortality rate in zebrafish. The results align with existing literature, indicating that elevated concentrations of herbal substances frequently correspond with increased toxicity.

Table 2: Cumulative mortality of zebrafish at different concentrations of nanoherbal *C. surinamense* leaves over time.

Concentrations (mg/L)	Count of Zebrafish	Total Percentage of Zebrafish Deaths at Different Intervals Times				Cumulative Mortality (%)
		24 h	48 h	72 h	96 h	
Control	10	0%	0%	0%	0%	0
12.5	10	0%	0%	0%	0%	0
25	10	0%	0%	0%	0%	0
50	10	0%	0%	0%	0%	0
100	10	0%	0%	0%	0%	0
200	10	0%	0%	0%	10%	10%
400	10	0%	0%	10%	20%	40%
800	10	0%	20%	10%	40%	70%
LC50 (mg/L)		-	2225.85	3300.059	990.617	516.867

3.3 *Histopathological evaluation*

3.3.1 Brain

The brain tissue structure of the zebrafish in the control group (B1) and at lower doses (12.5, 25, 50, and 100 mg/L) shows no signs of toxicity or significant histopathological changes (Figure 5(B1)–(B5). The histological structure remains intact, characterised by normal brain cells and no cell damage or inflammation. However, significant histological alterations were detected at increased concentrations (200–800 mg/L), especially in Purkinje cells, which are critical for motor coordination. At dose concentrations of 400 and 800 mg/L, early changes include cytoplasmic swelling and karyolysis (nuclear damage) in Purkinje cells, indicating severe structural damage (Figure 5(B6)–(B8)). This damage is probably caused by oxidative stress from the nanoherbal *C. surinamense* leaves, which can generate free radicals that harm cell parts. In addition, long-term use of high quantities of the leaves might cause mild inflammation and changes to the brain's metabolism, leading to cell damage [38], [39].

At the maximum dosage of 800 mg/L, Purkinje cell impairment intensifies in the zebrafish, resulting in the considerable loss and atrophy of these cells. This is likely attributable to apoptosis or programmed cell death, resulting from metabolic imbalances or genetic damage. Purkinje cell apoptosis was recognised as a marker of toxicity and was characterised by specific histological alterations, including cell shrinkage, chromatin condensation, nuclear fragmentation, and the formation of apoptotic bodies, which were subsequently phagocytosed by surrounding cells [40], [41]. The significant reduction in Purkinje cells at high doses indicates severe structural damage to brain tissue, which could lead to severe motor impairment. More importantly, this damage reflects the acute toxicity potential of nanoherbal *C. surinamense* leaves, which can disrupt the neurological function of zebrafish; this suggests that prolonged exposure to high doses may cause functional damage to the central nervous system [42].

3.3.2 Liver

Based on the toxicity tests of the nanohebal *C. surinamense* leaves at doses of 0, 12.5, 25, 50, 100, 200, 400, and 800 mg/L, toxic effects appear at doses ranging from 100 to 800 mg/L. The test animals show normal liver conditions at the control dose (0 mg/L), with regular hepatocytes and an evenly distributed cytoplasm with no pathological changes. In the control and at doses of 12.5, 25, and 50 mg/L, no significant signs of toxicity were observed, with the liver of the test animals remaining in normal condition (Figure 6(L1)–(L4)). However, at a dose of 100 mg/L, although no mortality was observed in the zebrafish, slight liver changes start to appear, involving, for example, tissue disorganisation, cytosolic heterogeneity, and nuclear eccentricity, indicating early signs of toxicity. The toxic effects were more pronounced at doses between 200 and 800 mg/L, as illustrated in Figure 6(L5)–(L8). The observed damage includes cytosolic vacuolisation, the loss of cell boundaries, necrosis, and the release of cytosolic contents between liver cells. The administration of doses of 400 and 800 mg/L results in notable liver damage, characterised by necrotic appearances that suggest severe cellular injury; this may contribute to more serious liver dysfunction [43], [44].

Preliminary signs of liver toxicity were observed at 100 mg/L and progressively worsened with increasing doses, though no fatality was induced in the zebrafish. These findings correspond with previous studies demonstrating that high dosages of certain chemicals can cause tissue disorganisation, necrosis, and liver cell damage while not resulting in mortality [35], [43], [44], [45]. The histological changes depicted in Figure 6(L1)–(L8) indicate the progressive degeneration of liver tissue with increasing dosage, with more pronounced necrosis at higher doses. These results confirm the potential toxicity of nanoherbal *C. surinamense* leaves and their increase with dosage; thus, further studies are required to support the use of these leaves in therapeutic or other applications.

3.3.3 Intestine

According to the histopathological analysis of the zebrafish intestines, the administration of nanoherbal *C. surinamense* leaves results in significantly varied levels of tissue damage, contingent upon the concentration of the dose. The groups receiving low doses of 12.5 and 25 mg/L (Figure 7(U2) and (U3)) exhibit mild inflammation, accompanied by moderate leucocyte infiltration, with the villi tissue showing no significant structural damage. Normal intestinal histology was determined by the presence of goblet cells, which maintain their typical structure. Further, the intestinal histology of the villi remains intact, with no indication of significant damage [46]. Histological damage is evident at a concentration of 50 mg/L, as illustrated in Figure 7(U4), characterised by partial villous rupture and increased leucocyte infiltration. At a concentration of 100 mg/L, significant tissue damage and histological changes can be observed, characterised by numerous disrupted villi and substantial damage to the tissue structure. A significant increase in intestinal histopathological damage can be noted in the high-dose groups of 200, 400, and 800 mg/L (Figure 7(U6)–(U8)). Tissue damage starts at a concentration of 200 mg/L, characterised by histological changes to villi and increased leucocyte infiltration, resulting in tissue inflammation. At a dose of 400 mg/L, the histological damage increases, with significant leucocyte infiltration and severe villus injury, thereby impairing the intestinal absorption performance. The administration of the high dose of 800 mg/L can lead to considerable tissue damage, marked by a near-total loss of normal intestinal tissue, notable villus fragmentation, and prominent leucocyte infiltration, exacerbating the tissue injury [43], [47].

The study findings indicate that the severity of the toxicological and histopathological effects on the intestinal tissue of zebrafish depends on the level of exposure to, or dose of nanoherbal *C. surinamense* leaves. High-dose administration, particularly at 400 and 800 mg/L, was known to cause significant oxidative stress, leading to the excessive formation of reactive oxygen species (ROS). These ROS were not only capable of damaging cell membranes, proteins, and DNA but were also significantly accumulated in intestinal tissue, resulting in villus fragmentation, extensive leucocyte infiltration, and the disruption of the normal intestinal tissue structure [46], [48], [49].

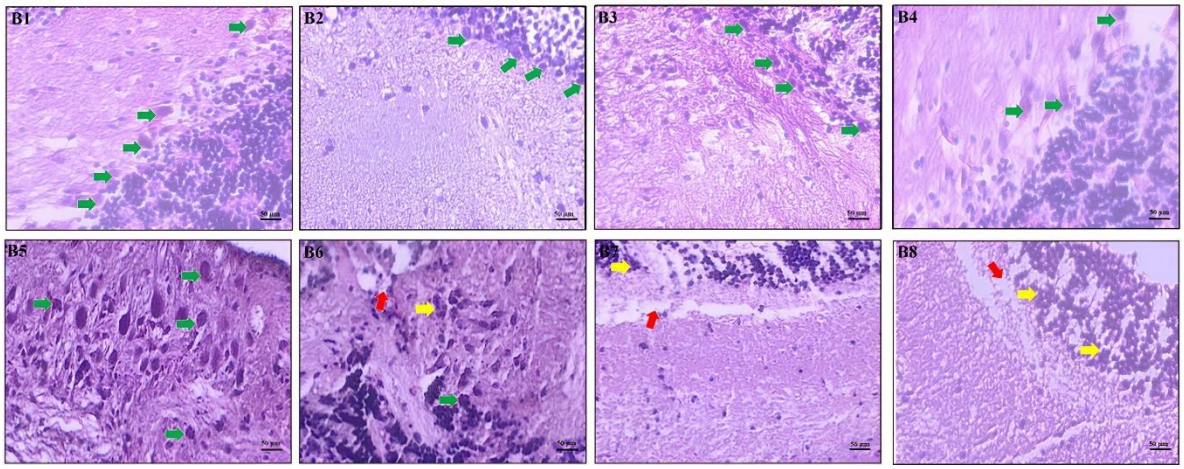

Figure 5: Histological analysis of zebrafish brain at different treatment doses: (B1) control (0 mg/L), (B2) 12.5 mg/L, (B3) 25 mg/L, (B4) 50 mg/L, (B5) 100 mg/L, (B6) 200 mg/L, (B7) 400 mg/L, (B8) 800 mg/L. Yellow arrows indicate Purkinje cells, while red arrows highlight histological damage. Yellow areas denote necrosis in brain tissue. H&E at 40x magnification.

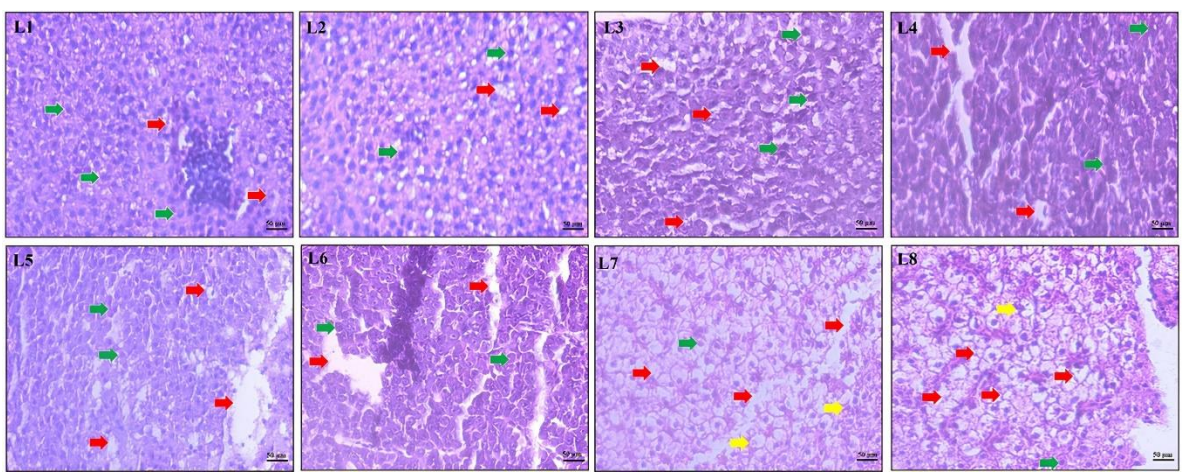

Figure 6: Histopathology of zebrafish liver at different treatment doses: (L1) Control (0 mg/L), (L2) 12.5 mg/L, (L3) 25 mg/L, (L4) 50 mg/L, (L5) 100 mg/L, (L6) 200 mg/L, (L7) 400 mg/L, (L8) 800 mg/L. The green arrow indicates normal hepatocytes, the red arrow indicates cytoplasmic vacuolation, and the yellow arrow indicates necrosis. H&E at 40x magnification.

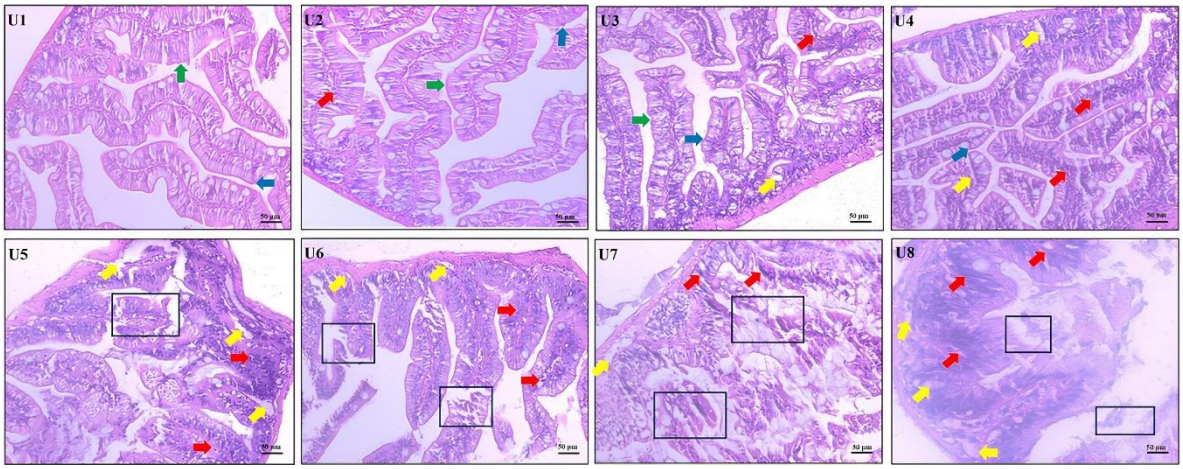

Figure 7: Histopathology of zebrafish intestines at different treatment doses: (U1) Control (0 mg/L), (U2) 12.5 mg/L, (U3) 25 mg/L, (U4) 50 mg/L, (U5) 100 mg/L, (U6) 200 mg/L, (U7) 400 mg/L, (U8) 800 mg/L, where the green arrow indicates normal goblet cells, blue arrow points to the villi, red arrow shows leukocyte infiltration, yellow arrow highlights a tear in the villi, and the square and yellow arrow indicate severe damage in the intestine histology. H&E at 40x magnification.

4 Conclusions

The leaves of nanoherbal Jopan (*C. surinamense*) exhibit considerable potential for future applications in herbal medicine. Analyses using ProTox 3.0 and molecular docking of the CYP450 protein have revealed that 2-cyclopentene-1-undecanoic acid derived from Jopan leaves is highly toxic, with a lethal dose of 48 mg/kg. Additionally, 2-undecanone 2,4-dinitrophenylhydrazone demonstrated a strong binding affinity for zebrafish, with a binding strength of –7.4 kcal/mol, indicating potential harmful effects. *In vivo* experiments on zebrafish classified the nanoherbal as slightly toxic, with an LC50 value of 516.87 mg/L at 96 hours. Histopathological analysis indicated safety up to 200 mg/L, with no observable signs of toxicity; however, at elevated concentrations (400 and 800 mg/L), significant histological damage was observed in vital organs, suggesting an increased risk of toxicity. This study offers valuable insights into the safety profile of nanoherbal Jopan, which could inform the development of safer herbal medicines and contribute to the formulation of more effective herbal products with appropriate toxicity considerations for human safety.

Acknowledgments

We gratefully acknowledge the financial support provided for the second year of this research in 2025 by the Research Funding Program of the Directorate of Research and Community Service (DPPM), Ministry of Higher Education, Science, and Technology of the Republic of Indonesia (Kemdiktisaintek), through the PMDSU Batch VII postgraduate research scheme (Contract No. 75/UN5.4.10.K/PT.01.03/KT-DPPM/2025).

Author Contributions

S.I.: conceptualization, investigation, reviewing and editing, corresponding author; D.P.W.: investigation, methodology, research data collection, data analysis, writing original draft; E.: research design, project administration, writing, reviewing and editing; and Y.H.M.: conceptualization, data curation, writing, reviewing and editing. All authors have read and accepted the published version of the work.

Conflicts of Interest

The authors declared that they had no conflicts of interest.

References

[1] S. Kaushal, N. Priyadarshi, P. Garg, N. K. Singhal, and D. K. Lim, "Nano-biotechnology for bacteria identification and potent anti-bacterial properties: A review of current state of the art," *Nanomaterials*, vol. 13, no. 2529, pp. 1–25, 2023.

[2] E. K. Sher, M. Alebić, M. M. Boras, E. Boškailo, E. K. Farhat, A. Karahmet, B. Pavlović, F. Sher, and L. Lekić, "Nanotechnology in medicine revolutionizing drug delivery for cancer and viral infection treatments," *International Journal of Pharmaceutics*, vol. 660, 2024, Art. no. 124345.

[3] X. Han, K. Xua, O. Taratulab, and K. Farsadc, "Applications of nanoparticles in biomedical imaging," *Nanoscale*, vol. 11, no. 3, pp. 799–819, 2019.

[4] C. G. P. Rumahorbo, S. Ilyas, S. Hutahaean, and C. F. Zuhra, "*Bischofia javanica* and *Phaleria macrocarpa* nano herbal combination on blood and liverkidney biochemistry in oral dquamous cell carcinoma-induced rats," *Pharmacia*, vol. 71, pp. 1–8, 2024.

[5] P. C. Situmorang, S. Ilyas, S. Hutahaean, and R. Rosidah, "Components and acute toxicity of nanoherbal haramonting (*Rhodomyrtus tomentosa*)," *Journal of HerbMed Pharmacology*, vol. 10, no. 1, pp. 139–148, 2021.

[6] A. Hussain, F. Attique, S. A. R. Naqvi, A. Ali, M. Ibrahim, H. Hussain, F. Zafar, R. S. Iqbal, M. A. Ayub, M. A. Assiri, M. Imran, and S. Ullah, "Nanoformulation of curcuma longa root extract and evaluation of its dissolution potential," *ACS Omega*, vol. 8, no. 1, pp. 1088–1096, 2023.

[7] T. Teame, Z. Zhang, C. Ran, H. Zhang, Y. Yang, Q. Ding, M. Xie, C. Gao, Y. Ye, M. Duan, and Z. Zhou, "The use of zebrafish (*Danio rerio*) as biomedical models," *Animal Frontiers*, vol. 9, no. 3, pp. 68–77, 2019.

[8] S. S. Balan, P. Manokaram, S. Maya, H. Bahari, M. M. Uzid, M. Danial, A. Z. Abidin, A. D. Jesus, and M. Rahmadi, "Evaluation an aqueous extract of irradiated and non irradiated of Orthosiphon aristatus on zebrafish embryo (*Danio rerio*) through acute toxicity assay," *Trends in Sciences*, vol. 19, no. 14, p. 4980, 2022.

[9] S. K. Verma, A. Nandi, A. Sinha, P. Patel, S. Mohanty, E. Jha, S. Jena, P. Kumari, A. Ghosh, I. Jerman, R. S. Chouhan, A. Dutt, S. K. Samal, Y. K. Mishra, R. S. Varma, P. K. Panda, N. K. Kaushik, D. Singh, and M. Suar, "The posterity of zebrafish in paradigm of in vivo molecular toxicological profiling," *Biomedicine and Pharmacotherapy*, vol. 171, 2024, Art. no. 116160.

[10] J. Xavier and K. Kripasana, "Acute toxicity of leaf extracts of Enydra fluctuans Lour in zebrafish (*Danio rerio* Hamilton)," *Scientifica*, vol. 2020, pp. 1–6, 2020.

[11] M. D'amora, V. Raffa, F. D. Angelis, and F. Tantussi, "Toxicological profile of plasmonic nanoparticles in zebrafish model," *International Journal of Molecular Sciences*, vol. 22, no. 12, pp. 1–32, 2021.

[12] N. Tavvabi-Kashani, M. Hasanpour, V. B. Rahimi, N. Vahdati-Mashhadian, and V. R. Askari, "Pharmacodynamic, pharmacokinetic, toxicity, and recent advances in Eugenol's potential benefits against natural and chemical noxious agents: A mechanistic review," *Toxicon*, vol. 238, 2024, Art. no. 107607.

[13] J. J. Li, Y. X. Yue, S. J. Shi, and J. Z. Xue, "Investigation on toxicity mechanism of halogenated aromatic disinfection by-products to zebrafish based on molecular docking and QSAR model," *Chemosphere*, vol. 341, 2023, Art. no. 139916.

[14] W. Sents, E. Ivanova, C. Lambrecht, D. Haesen, and V. Janssens, "The biogenesis of active protein phosphatase 2A holoenzymes: A tightly regulated process creating phosphatase specificity," *FEBS Journal*, vol. 280, no. 2, pp. 644–661, 2013.

[15] F. P. Guengerich, "A history of the roles of cytochrome P450 enzymes in the toxicity of drugs," *Toxicological Research*, vol. 37, no. 1, pp. 1–23, 2021.

[16] K. Fujii, K. Yamakawa, Y. Takeda, N. Okuda, A. Takasu, and F. Ono, "Understanding the pathophysiology of acute critical illness: Translational lessons from zebrafish models," *Intensive Care Medicine Experimental*, vol. 12, no. 8, pp. 1–8, 2024.

[17] D. P. Wati, S. Ilyas, and D. Khairani, "In silico study of compounds from nanoherbal Jopan (*Clibadium surinamense* L.) leaves as inhibitors AKT1 interaction," *Trends in Sciences*, vol. 22, no. 1, p. 8729, 2024.

[18] H. A. Alomar, W. M. El Kady, A. A. Mandour, A. A. Naim, N. I. Ghali, T. A. Ibrahim, and N. Fathallah, "Computational antidiabetic assessment of *Salvia splendens* L. polyphenols: SMOTE, ADME, ProTox, docking, and molecular dynamic studies," *Results in Chemistry*, vol. 14, 2025, Art. no. 102081.

[19] W. Nafisah, F. Fatchiyah, M. H. Widyananda, Y. I. Christina, M. Rifa'I, N. Widodo, and M. S. Djati, "Potential of bioactive compound of

Cyperus rotundus L. rhizome extract as inhibitor of PD-L1/PD-1 interaction: An in silico study," *Agriculture and Natural Resources*, vol. 56, no. 4, pp. 751–760, 2022.

[20] P. S. Pallan, L. D. Nagy, L. Lei, E. Gonzalez, V. M. Kramlinger, C. M. Azumaya, Z. Wawrzak, M. R. Waterman, F. P. Guengerich, and M. Egli, "Structural and kinetic basis of steroid 17α,20-lyase activity in Teleost fish cytochrome P450 17A1 and its absence in cytochrome P450 17A2," *Journal of Biological Chemistry*, vol. 290, no. 6, pp. 3248–3268, 2015.

[21] H. Rasyid and R. Armunanto, "Molecular docking analysis on epidermal growth factor receptor wild type (EGFR wt) with quinazoline derivative compounds as tyrosine kinase inhibitors," *Applied Science and Engineering Progress*, vol. 10, no. 4, pp. 293–299, 2017, doi: 10.14416/j.ijast.2017.12.001.

[22] Y. H. Prayogo, A. W. Anggini, A. Carolina, E. G. T. Manurung, R. K. Sari, A. Purwoko, and G. Pasaribu, "In vitro and In silico antibacterial potency of eucalyptus leaf oil from hybrid clones of *E. grandis* with *E. urophylla* and *E. pellita*," *Applied Sciences and Engineering Progress*, vol. 18, no. 3, 2025, Art. no. 7671, doi: 10.14416/j.asep.2025.01.002.

[23] OECD, *OECD TG 453: Testing of Chemicals Combined Chronic Toxicity/Carcinogenicity Studies*, 2018.

[24] A. Augustine and J. Xavier, "Toxicological evaluation of ethanolic leaf and fruit extracts of *Phaseolus vulgaris* L. treated with wastewater in Danio rerio hamilton (zebrafish)," *Asian Journal of Plant Sciences*, vol. 21, no. 1, pp. 24–31, 2022.

[25] S. Alam, G. Afzal, R. Hussain, H. M. Ali, A. Sami, R. M. Malik, R. Jabeen, F. S. Ataya, and K. Li, "Estimation of median LC50 and toxicity of environmentally relevant concentrations of thiram in Labeo rohita," *npj Clean Water*, vol. 8, no. 1, p. 9, 2025.

[26] M. G. Shinde, S. J. Modi, and V. M. Kulkarni, "Synthesis, pharmacological evaluation, molecular docking and in silico ADMET prediction of nitric oxide releasing biphenyls as anti-inflammatory agents," *Journal of Applied Pharmaceutical Science*, vol. 7, no. 10, pp. 37–47, 2017.

[27] K. Jurowski and A. Krośniak, "Prediction of key toxicity endpoints of AP-238 a new psychoactive substance for clinical toxicology and forensic purposes using in silico methods," *Scientific Reports*, vol. 14, no. 1, 2024, Art. no. 28977.

[28] J. Bercu *et al.*, "A cross-industry collaboration to assess if acute oral toxicity (Q)SAR models are fit-for-purpose for GHS classification and labelling," *Regulatory Toxicology and Pharmacology*, vol. 120, 2021, Art. no. 104843.

[29] A. Balkrishna, S. Pokhrel, H. Singh, M. Joshi, V. P. Mulay, S. Haldar, and A. Varshney, "Withanone from *withania somnifera* attenuates sars-cov-2 rbd and host ace2 interactions to rescue spike protein induced pathologies in humanized zebrafish model," *Drug Design, Development and Therapy*, vol. 15, pp. 1111–1133, 2021.

[30] S. Y. Khan, M. A. Rather, A. Shah, I. Ahmad, I. Ahmad, K. K. Saba, and F. R. Sofi, "Exploring 3D structure of gonadotropin hormone receptor using homology modeling, molecular dynamic simulation and docking studies in rainbow trout, Oncorhynchus mykiss," *Endocrine and Metabolic Science*, vol. 15, 2024, Art. no. 100171.

[31] J. Zheng, T. Lin, and W. Chen, "Removal of the precursors of N-nitrosodiethylamine (NDEA), an emerging disinfection byproduct, in drinking water treatment process and its toxicity to adult zebrafish (Danio rerio)," *Chemosphere*, vol. 191, pp. 1028–1037, 2018.

[32] C. E. Enyoh, Q. Wang, P. E. Ovuoraye, and T. O. Maduka, "Toxicity evaluation of microplastics to aquatic organisms through molecular simulations and fractional factorial designs," *Chemosphere*, vol. 308, 2022, Art. no. 136342.

[33] C. Vicidomini, R. Palumbo, M. Moccia, and G. N. Roviello, "Oxidative processes and xenobiotic metabolism in plants: Mechanisms of defense and potential therapeutic implications," *Journal of Xenobiotics*, vol. 14, no. 4, pp. 1541–1569, 2024.

[34] P. Gupta, A. Mahapatra, A. Suman, and R. K. Singh, "In silico and in vivo assessment of developmental toxicity, oxidative stress response & Na+/K+-ATPase activity in zebrafish embryos exposed to cypermethrin," *Ecotoxicology and Environmental Safety*, vol. 251, 2023, Art. no. 114547.

[35] Y. L. dos Santos Melo, A. C. Luchiari, B. S. Lopes, M. G. F. R. Silva, T. dos Santos Pais, J. E. P. G. Cortez, C. da Silva Camillo, S. A.

Bezerra de Moura, J. K. da Silva-Maia, and A. H. de Araújo Morais, "Acute toxicity of trypsin inhibitor from tamarind seeds in embryo and adult zebrafish (*Danio rerio*)," *Toxicology Reports*, vol. 13, 2024, Art. no. 101766.

[36] R. de Carvalho Rocha Koga, G. Custodio de Souza, A. V. Tavares de Lima Teixeira, A. M. Ferreira, B. L. Sánchez-Ortiz, L. Silva Abreu, J. F. Tavares, and J. C. T. Carvalho, "Hydroethanolic extracts from *Bauhinia guianensis*: A study on acute toxicity in zebrafish embryos and adults," *Pharmaceutical Biology*, vol. 62, no. 1, pp. 577–591, 2024.

[37] R. Fakhlaei, J. Selamat, A. F. Abdull Razis, R. Sukor, S. Ahmad, A. Khatib, and X. Zou, "Development of a zebrafish model for toxicity evaluation of adulterated *Apis mellifera* honey," *Chemosphere*, vol. 356, Art. no. 141736, 2024.

[38] D. L. Zhang, C. X. Hu, D. H. Li, and Y. D. Liu, "Lipid peroxidation and antioxidant responses in zebrafish brain induced by Aphanizomenon flos-aquae DC-1 aphantoxins," *Aquatic Toxicology*, vol. 144–145, pp. 250–256, 2013.

[39] N. Jiang, P. Song, X. Li, L. Zhu, J. Wang, X. Yin, and J. Wang, "Dibutyl phthalate induced oxidative stress and genotoxicity on adult zebrafish (*Danio rerio*) brain," *Journal of Hazardous Materials*, vol. 424, 2022, Art. no. 127749.

[40] E. Paduraru, R. Jijie, I. A. Simionov, C. M. Gavrilescu, T. Ilie, D. Iacob, A. Lupitu, C. Moisa, C. Muresan, L. Copolovici, D. M. Copolovici, G. Mihalache, F. D. Lipsa, G. Solcan, G. A. Danelet, M. Nicoara, A. Ciobica, and C. Solcan, "Honey enriched with additives alleviates behavioral, oxidative stress, and brain alterations induced by heavy metals and imidacloprid in zebrafish," *International Journal of Molecular Sciences*, vol. 25, no. 21, 2024, Art. no. 11730.

[41] M. Fricker, A. M. Tolkovsky, V. Borutaite, M. Coleman, and G. C. Brown, "Neuronal cell death," *Physiological Reviews*, vol. 98, no. 2, pp. 813–880, 2018.

[42] L. Gence, D. Fernezelian, M. Bringart, B. Veeren, A. Christophe, F. Brion, O. Meilhac, J. L. Bascands, and N. Diotel, "*Hypericum lanceolatum* Lam. medicinal plant: Potential toxicity and therapeutic effects based on a zebrafish model," *Frontiers in Pharmacology*, vol. 13, 2022, Art. no. 832928.

[43] J. C. T. Carvalho, G. C. De Souza, I. D. R. Da Silva, M. D. Viana, N. C. De Melo, B. L. Sánchez-Ortiz, M. M. R. De Oliveira, W. R. Barbosa, and I. M. Ferreira, "Acute toxicity of the hydroethanolic extract of the flowers of *Acmella oleracea* l. in zebrafish (*Danio rerio*): Behavioral and histopathological studies," *Pharmaceuticals*, vol. 12, no. 4, p. 173, 2019.

[44] D. S. Omnes, J. Xavier, and A. Suresh, "Assessing oral acute toxicity and histopathological effects of *Strelitzia reginae* Aiton leaf extracts in Zebrafish (*Danio rerio* Hamilton)," *Plant Science Today*, vol. 11, no. 2, pp. 262–270, 2024.

[45] L. Ma, Z. Yin, Q. Xie, Y. Xu, Y. Chen, Y. Huang, Z. Li, X. Zhu, Y. Zhao, W. Wen, H. Xu, and X. Wu, "Metabolomics and mass spectrometry imaging reveal the chronic toxicity of indoxacarb to adult zebrafish (*Danio rerio*) livers," *Journal of Hazardous Materials*, vol. 453, p. 131304, 2023.

[46] F. Yu, Y. Liu, W. Wang, S. Yang, Y. Gao, W. Shi, H. Hou, J. Chen, and R. Guo, "Toxicity of TPhP on the gills and intestines of zebrafish from the perspectives of histopathology, oxidative stress and immune response," *Science of the Total Environment*, vol. 908, 2024, Art. no. 168212.

[47] F. H. Holanda, A. N. Ribeiro, B. L. Sánchez-Ortiz, G. C. de Souza, S. F. Borges, A. M. Ferreira, A. C. Florentino, S. A. Yoshioka, L. S. Moraes, J. C. T. Carvalho, and I. M. Ferreira, "Anti-inflammatory potential of baicalein combined with silk fibroin protein in a zebrafish model (*Danio rerio*)," *Biotechnology Letters*, vol. 45, no. 2, pp. 235–253, 2023.

[48] A. A. de Souza, B. L. S. Ortíz, S. F. Borges, A. V. P. Pinto, R. da S. Ramos, I. C. Pena, R. D. C. R. Kago, C. E. Batista, G. C. de Souza, A. M. Ferreira, S. D. Junior, and J. C. T. Carvalho, "Acute toxicity and anti-inflammatory activity of *Trattinnickia rhoifolia* Willd (Sucuruba) using the *zebrafish* model," *Molecules*, vol. 27, no. 22, p. 7741, 2022.

[49] J. Zhang, Q. Chen, Y. Wang, R. Wang, R. Wang, X. Hao, Y. Zheng, X. An, and J. Qi, "Protective effects of feruloyl oligosaccharides from fermented wheat bran againsoxidative stress in IPEC-J2 cells in vitro and in a zebrafish model in vivo," *Journal of Food Quality*, vol. 2022, no. 1, 2022, Art. no. 8001728.